

# The lepton–flavour violating decay $\tau \rightarrow \mu\mu\bar{\mu}$ at the LHC

M. Giffels<sup>1</sup>, J. Kallarackal<sup>2,3</sup>, M. Krämer<sup>2</sup>, B. O’Leary<sup>2</sup>, and A. Stahl<sup>1</sup>

<sup>1</sup> *III. Physikalisches Institut, RWTH Aachen, 52056 Aachen, Germany*

<sup>2</sup> *Institut für Theoretische Physik, RWTH Aachen, 52074 Aachen, Germany*

<sup>3</sup> *Institut für Physik, Humboldt–Universität zu Berlin, 12489 Berlin, Germany*

## Abstract

Lepton–flavour violating  $\tau$ –decays are predicted in many extensions of the Standard Model at a rate observable at future collider experiments. In this article we focus on the decay  $\tau \rightarrow \mu\mu\bar{\mu}$ , which is a promising channel to observe lepton–flavour violation at the Large Hadron Collider LHC. We present analytic expressions for the differential decay width derived from a model–independent effective Lagrangian with general four–fermion operators, and estimate the experimental acceptance for detecting the decay  $\tau \rightarrow \mu\mu\bar{\mu}$  at the LHC. Specific emphasis is given to decay angular distributions and how they can be used to discriminate new physics models. We provide specific predictions for various extensions of the Standard Model, including supersymmetric, little Higgs and technicolour models.

# 1 Introduction

In the Standard Model (SM) with massless neutrinos, lepton flavour is conserved. However, the current neutrino oscillation data indicate non-degenerate neutrinos with large mixing angles [1], and this, in turn, implies lepton-flavour violation (LFV) within the SM extended to include massive neutrinos. This flavour violation is large in the neutrino sector (where the Pontecorvo–Maki–Nakagawa–Sakata (PMNS) mixing matrix has large off-diagonal entries, unlike the Cabbibo–Kobayashi–Maskawa (CKM) matrix of the quark sector), but very small in the charged-lepton sector, with branching ratios for LFV decays suppressed by factors of  $\delta m_\nu^2/m_W^2$  [2], and thus well below current and future experimental limits. Hence, any experimental signal of charged-lepton-flavour violation would be a clear indication of physics beyond the SM. While current bounds from non-collider experiments strongly constrain  $\mu \rightarrow e$  transitions, the limits on  $\tau \rightarrow \mu$  and  $\tau \rightarrow e$  conversion are much less stringent [1]. Moreover, as we shall discuss in detail below, many extensions of the SM predict LFV in  $\tau$  decays at a rate accessible at future  $e^+e^-$  and hadron colliders.

In this article we focus on the decay  $\tau \rightarrow \mu\mu\bar{\mu}$  which should provide a clean signature to observe LFV at the Large Hadron Collider LHC [3].<sup>1</sup> In general, the decay  $\tau \rightarrow ee\bar{e}$  would have similar characteristics, though in many models (including several of the models we consider), the couplings to electrons are suppressed relative to the couplings to muons. Moreover, muons provide a far cleaner signal than electrons in a hadron collider environment [3]. At the LHC,  $\tau$  leptons are produced predominantly from decays of  $B$  and  $D$  mesons and  $W$  and  $Z$  bosons. In the low-luminosity phase, corresponding to an integrated luminosity of  $10 \text{ fb}^{-1}$  per year, one expects approximately  $2 \times 10^{12}$  and  $2 \times 10^8$   $\tau$  leptons produced per year from heavy meson and weak boson decays, respectively. The  $\tau$  leptons from heavy meson decays result in a much softer muon transverse momentum spectrum and are more difficult to trigger and analyze. Therefore, in our Monte Carlo studies we only include  $\tau$  leptons from  $W$  and  $Z$  boson decays. With standard acceptance cuts ( $|\eta_\mu| < 2.5$  and  $p_{T,\mu} > 3 \text{ GeV}$ ), and requiring either two muons with  $p_T > 7 \text{ GeV}$  or a single muon with  $p_T > 19 \text{ GeV}$  for trigger purposes, we find acceptances for various BSM models of approximately 25–30%. Thus, even restricting ourselves to  $\tau$  leptons from weak boson decays only, and assuming a branching ratio close to the current upper limit  $\text{BR}(\tau \rightarrow \mu\mu\bar{\mu}) \leq 1.9 \times 10^{-7}$  [1], we can expect approximately  $2 \times 10^8 \times 25\% \times 1.9 \times 10^{-7} \simeq 10$   $\tau \rightarrow \mu\mu\bar{\mu}$  events within the acceptance range of a typical LHC general purpose detector after one year of low-luminosity running. With  $30 \text{ fb}^{-1}$  of data, it should be possible to probe branching ratios down to a level of  $\text{BR}(\tau \rightarrow \mu\mu\bar{\mu}) \approx 10^{-8}$  [3, 6] at the LHC. [Recent results from  $B$  factories also begin to test branching ratios down to the level of  $5 \times 10^{-8}$  [7]; a prospective super B facility [8] could probe branching ratios of  $\mathcal{O}(10^{-10})$ .]

Note that there is an even tighter experimental limit on the radiative LFV decay  $\tau \rightarrow \mu\gamma$ , with

---

<sup>1</sup>LFV can also be probed at a future  $e^+e^-$  linear collider [4] and at muon or neutrino factories [5].

an upper bound on the branching ratio of  $\text{BR}(\tau \rightarrow \mu\gamma) \leq 6.8 \times 10^{-8}$  [1]. The radiative decay itself is difficult to detect at the LHC [3], and any model that allows the decay  $\tau \rightarrow \mu\mu\bar{\mu}$  to proceed through an effective  $\tau\mu\gamma$  vertex only is already constrained by this bound, and will be further suppressed by a factor of  $\alpha$  from the  $\bar{\mu}\mu\gamma$  vertex. However, models where the LFV  $\tau$  decay can be mediated by the exchange of new heavy particles escape the tight bound on radiative transitions. With this in mind, we will only investigate models of this type, though we will briefly comment on other models afterwards.

There are many observables associated with the decay  $\tau \rightarrow \mu\mu\bar{\mu}$ . Since we are focusing on models where the virtual particles have large masses  $M \gg m_\tau$ , the propagators are replaced by  $-i/M^2$ , and the obvious difference between models is the chiral structure of the effective vertices. We choose the angle  $\Theta$  to be the angle between the polarization of the  $\tau$  lepton and the momentum of the anti-muon (assuming  $\tau^- \rightarrow \mu^- \mu^- \mu^+$ ) and differentiate models according to their partial decay width in  $\cos \Theta$ , having integrated over all other kinematic variables. Approximately 85% of the  $\tau$  leptons from electroweak gauge bosons will be produced in  $W$  decays, which result in characteristic spin patterns. For example, the decay  $W^- \rightarrow \tau^- \bar{\nu}_\tau$  produces  $\tau$  leptons with left-handed helicity only, so that the polarization vector is antiparallel to the momentum vector and can thus be determined experimentally. We note that the polarization of  $\tau$  leptons from  $D$  and  $B$  mesons or from  $Z$  decays cannot be determined in such simple manner. The  $\tau$  leptons from these sources should thus not be included in our polarization analysis, but instead dilute the signal.

The paper is organized as follows: first, we will present analytic expressions for the matrix element and differential decay width derived from an effective Lagrangian with the most general four-fermion  $(\bar{\mu}\mu)(\bar{\mu}\tau)$  interactions that do not involve derivatives. The result of this calculation has been used in a Monte Carlo study to estimate the detector acceptance for various new physics models. In order to show how the decay angular distribution can be employed to discriminate between different models we provide specific predictions for various supersymmetric, little Higgs and technicolour models, and models with doubly charged Higgs bosons. In each case, we will briefly describe the relevant features of the model, extract the values for the effective parameters of the general matrix element and differential decay width expressions, present the dependence of its partial decay width with respect to  $\cos \Theta$  and the acceptance for the decay simulated in a typical LHC general purpose detector with the experimental cuts described above. Finally, we will briefly discuss three additional classes of models: those that fit the criterion of heavy mediating particles, but have no concrete predictions for the dependence on  $\cos \Theta$ , those which are very constrained by the  $\tau \rightarrow \mu\gamma$  data, and unparticle models.

## 2 Model-independent analysis

We consider an interaction using effective four-fermion vertices. Derivatives have not been included, since by the equations of motion these derivatives will be of the order of the lepton masses, which should

be small in comparison to the scale of the new physics. For other model-independent investigations based on effective lepton-flavour-violating interactions, see Refs. [9].

The effective Lagrangian is given by (using  $\rho$  and  $\nu$  as Lorentz indices to avoid confusion with the symbol  $\mu$  being used for muon spinors)

$$\begin{aligned}
\mathcal{L} &= G \left( g_{LL}^S (\bar{\mu} P_R \mu) (\bar{\mu} P_L \tau) + g_{LR}^S (\bar{\mu} P_R \mu) (\bar{\mu} P_R \tau) + g_{RL}^S (\bar{\mu} P_L \mu) (\bar{\mu} P_L \tau) + g_{RR}^S (\bar{\mu} P_L \mu) (\bar{\mu} P_R \tau) \right. \\
&\quad + g_{LL}^V (\bar{\mu} \gamma_\nu P_R \mu) (\bar{\mu} \gamma^\nu P_L \tau) + g_{LR}^V (\bar{\mu} \gamma_\nu P_R \mu) (\bar{\mu} \gamma^\nu P_R \tau) \\
&\quad + g_{RL}^V (\bar{\mu} \gamma_\nu P_L \mu) (\bar{\mu} \gamma^\nu P_L \tau) + g_{RR}^V (\bar{\mu} \gamma_\nu P_L \mu) (\bar{\mu} \gamma^\nu P_R \tau) \\
&\quad \left. + g_{LR}^T \left( \bar{\mu} \frac{\sigma^{\rho\nu}}{\sqrt{2}} P_R \mu \right) \left( \bar{\mu} \frac{\sigma^{\rho\nu}}{\sqrt{2}} P_R \tau \right) + g_{RL}^T \left( \bar{\mu} \frac{\sigma^{\rho\nu}}{\sqrt{2}} P_L \mu \right) \left( \bar{\mu} \frac{\sigma^{\rho\nu}}{\sqrt{2}} P_L \tau \right) \right) \\
&\equiv G \sum_{a,b,c} g_{ab}^c (\bar{\mu} \Gamma^c \gamma^0 P_a \gamma^0 \mu) (\bar{\mu} \Gamma^c P_b \tau) , \tag{1}
\end{aligned}$$

where  $P_{L/R}$  are the left- and right-handed projection operators, respectively, with  $P_{L/R} = (1 \mp \gamma^5)/2$ , and  $\sigma^{\rho\nu} = i[\gamma^\rho, \gamma^\nu]/2$ . The symbols  $g_{ab}^c$  denote the couplings for the various chiral structures, with  $c = S$  for scalar,  $V$  for vector,  $T$  for tensor, so that  $\Gamma^S = 1, \Gamma^V = \gamma^\nu, \Gamma^T = \sigma^{\rho\nu}/\sqrt{2}$ , and where  $a = \{L, R\}$  is the chirality of the anti-muon and  $b = \{L, R\}$  is the chirality of the  $\tau$  lepton. [The presence of the  $\gamma^0$  matrices on each side of  $P_a$  in the final line is to allow  $a$  to be the chirality of the outgoing anti-muon.] The overall constant  $G$  is dimensionful, with units of  $\text{GeV}^{-2}$ . We will use  $G$  to absorb any normalization of the couplings  $g_{ab}^c$  for any particular model, so that we can present the  $g_{ab}^c$  as integers where possible. Note that not all ten couplings are independent, as through Fierz identities one of the four-fermion terms can be written as a sum of one or more of the others. However, we choose to keep the extra term for convenience. The use of Fierz identities can also show that the omitted  $g_{LL}^T \left( \bar{\mu} \frac{\sigma^{\rho\nu}}{\sqrt{2}} P_R \mu \right) \left( \bar{\mu} \frac{\sigma^{\rho\nu}}{\sqrt{2}} P_L \tau \right)$  and  $g_{RR}^T \left( \bar{\mu} \frac{\sigma^{\rho\nu}}{\sqrt{2}} P_L \mu \right) \left( \bar{\mu} \frac{\sigma^{\rho\nu}}{\sqrt{2}} P_R \tau \right)$  terms are identically zero.

Noting that there is a pair of identical fermions in the final state, the transition matrix element is given by

$$\begin{aligned}
\mathcal{M} &= G \sum_{a,b,c} g_{ab}^c (\bar{u}(p_{\mu_A}) \Gamma^c \gamma^0 P_a \gamma^0 v(p_{\bar{\mu}}) \bar{u}(p_{\mu_B}) \Gamma^c P_b u(p_\tau) \\
&\quad - \bar{u}(p_{\mu_B}) \Gamma^c \gamma^0 P_a \gamma^0 v(p_{\bar{\mu}}) \bar{u}(p_{\mu_A}) \Gamma^c P_b u(p_\tau)) , \tag{2}
\end{aligned}$$

where  $A$  and  $B$  label the muons. While we sum over final-state spins when squaring the matrix element, we keep the information about the  $\tau$  polarization by using  $u(p_\tau) \bar{u}(p_\tau) = (\not{p}_\tau + m_\tau) \left( \frac{1 + \gamma^5 \not{n}}{2} \right)$ , where  $n^\nu$  is the polarization vector of the  $\tau$  lepton.

Squaring this matrix element and performing integrations over the phase space except for the anti-muon energy and the angle  $\Theta$  between the polarization of the  $\tau$  lepton and the momentum of the

anti-muon produces the result for the normalized double-differential decay width:

$$\frac{1}{\Gamma} \frac{d\Gamma}{dx d\cos\Theta} = \frac{6x^2(a + bx + c \cos\Theta + dx \cos\Theta)}{(4a + 3b)}, \quad (3)$$

with the approximation that the muons are massless. Here  $x = 2E_{\bar{\mu}}/m_{\tau}$  is the reduced energy of the anti-muon, and the coefficients  $a, b, c$  and  $d$  are given by

$$\begin{aligned} a &= 3|g_{LL}^S|^2 + 12|g_{LL}^V|^2 + 3|g_{LR}^S|^2 + 48|g_{LR}^V|^2 + 108|g_{LR}^T|^2 + 3|g_{RL}^S|^2 + 48|g_{RL}^V|^2 + 108|g_{RL}^T|^2 + 3|g_{RR}^S|^2 \\ &\quad + 12|g_{RR}^V|^2 - 12 \operatorname{Re}(g_{LL}^S g_{LL}^{V*} + g_{RR}^V g_{RR}^{S*}) - 36 \operatorname{Re}(g_{LR}^S g_{LR}^{T*} + g_{RL}^S g_{RL}^{T*}), \\ b &= -2|g_{LL}^S|^2 - 8|g_{LL}^V|^2 - 3|g_{LR}^S|^2 - 48|g_{LR}^V|^2 - 108|g_{LR}^T|^2 - 3|g_{RL}^S|^2 - 48|g_{RL}^V|^2 - 108|g_{RL}^T|^2 - 2|g_{RR}^S|^2 \\ &\quad - 8|g_{RR}^V|^2 + 8 \operatorname{Re}(g_{LL}^S g_{LL}^{V*} + g_{RR}^V g_{RR}^{S*}) + 36 \operatorname{Re}(g_{LR}^S g_{LR}^{T*} + g_{RL}^S g_{RL}^{T*}), \\ c &= |g_{LL}^S|^2 + 4|g_{LL}^V|^2 - 3|g_{LR}^S|^2 - 48|g_{LR}^V|^2 - 108|g_{LR}^T|^2 + 3|g_{RL}^S|^2 + 48|g_{RL}^V|^2 + 108|g_{RL}^T|^2 - |g_{RR}^S|^2 \\ &\quad - 4|g_{RR}^V|^2 + 36 \operatorname{Re}(g_{LR}^S g_{LR}^{T*} - g_{RL}^S g_{RL}^{T*}) - 4 \operatorname{Re}(g_{LL}^S g_{LL}^{V*} - g_{RR}^V g_{RR}^{S*}), \\ d &= -2|g_{LL}^S|^2 - 8|g_{LL}^V|^2 + 3|g_{LR}^S|^2 + 48|g_{LR}^V|^2 + 108|g_{LR}^T|^2 - 3|g_{RL}^S|^2 - 48|g_{RL}^V|^2 - 108|g_{RL}^T|^2 + 2|g_{RR}^S|^2 \\ &\quad + 8|g_{RR}^V|^2 - 36 \operatorname{Re}(g_{LR}^S g_{LR}^{T*} - g_{RL}^S g_{RL}^{T*}) + 8 \operatorname{Re}(g_{LL}^S g_{LL}^{V*} - g_{RR}^V g_{RR}^{S*}). \end{aligned} \quad (4)$$

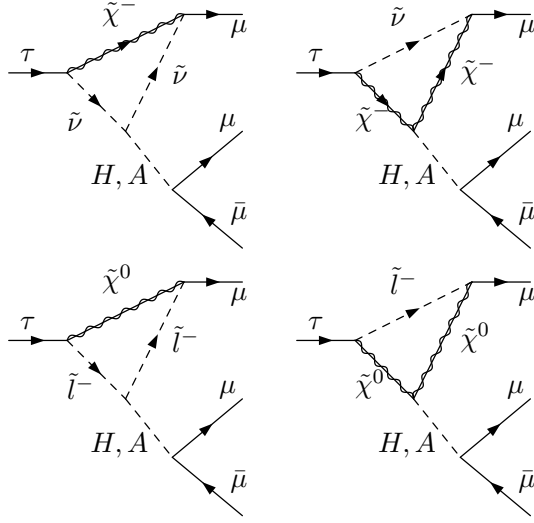
Hence the normalized differential decay width in  $\cos\Theta$  is

$$\frac{1}{\Gamma} \frac{d\Gamma}{d\cos\Theta} = \frac{1}{2} \left( 1 + \frac{4c + 3d}{4a + 3b} \cos\Theta \right), \quad (5)$$

where we use  $\Gamma$  to denote only the width of the  $\tau \rightarrow \mu\mu\bar{\mu}$  decay, to save on a proliferation of subscripts, rather than using it to denote the full  $\tau$  decay width. This normalized differential decay width is now independent of the absolute magnitudes of the four-fermion couplings. Muon mass effects are included in our full calculation. They are suppressed by powers of  $m_{\mu}/m_{\tau}$  and are thus numerically small.

### 3 Model Discrimination

Here we discuss various new physics models and consider how they may be discriminated using the distribution in  $\cos\Theta$ . Specifically, we consider the  $R$ -parity-conserving MSSM including see-saw neutrino masses at large  $\tan\beta$  [10, 11], the  $R$ -parity-violating MSSM [12], the Littlest Higgs model with  $T$ -parity [13], the topcolour-assisted technicolour model [14], the Higgs triplet model [15], and the Zee-Babu model [16]. The decays of  $\tau$  leptons to  $\mu\mu\bar{\mu}$  within each model have been discussed in the literature, but, as far as we are aware, only to the extent of predicting total branching ratios in terms of the model parameters, except for Ref. [17], which considers forward-backward asymmetries for the Higgs triplet and Zee-Babu models.



(plus diagrams with the muons crossed.)

Figure 1: Feynman diagrams leading to  $\tau \rightarrow \mu\mu\bar{\mu}$  in the see-saw MSSM with large  $\tan\beta$ .

### 3.1 Supersymmetric model with see-saw mechanism

Neutrino masses can be accommodated in the Minimal Supersymmetric Standard Model (MSSM) by adding singlet chiral superfields that have right-handed neutrino components and a large Majorana mass term, leading to the supersymmetric version of the “see-saw” mechanism [18, 19]. However, the see-saw MSSM allows for much stronger influence of the mixing in the neutrino sector on the charged lepton sector, through large renormalization-group effects in the slepton sector [20, 21]. Here, we focus on the potential for a large  $\tau \rightarrow \mu\mu\bar{\mu}$  branching ratio escaping the  $\tau \rightarrow \mu\gamma$  bound through an enhanced coupling of the MSSM Higgs bosons to muons for large  $\tan\beta$ , as proposed in Ref. [11]

We start directly from equation (15) in Ref. [11], which gives an effective coupling of the MSSM Higgs bosons to a  $\tau$  lepton and a muon. We reproduce it here for ease of reference:

$$\begin{aligned}
-\mathcal{L} &= (2G_F^2)^{1/4} \frac{m_\tau \kappa_{32}}{\cos^2\beta} (\bar{\tau}_R \mu_L) [\cos(\beta - \alpha) h^0 - \sin(\beta - \alpha) H^0 - iA^0] + \text{h.c.} \\
&= -(2G_F^2)^{1/4} m_\tau \kappa_{32} (\tan\beta)^2 (\bar{\tau} P_L \mu) [H^0 + iA^0] + \text{h.c.} \\
&= -(2G_F^2)^{1/4} m_\tau (\tan\beta)^2 [\kappa_{32} (\bar{\tau} P_L \mu) [H^0 + iA^0] + \kappa_{32}^* (\bar{\mu} P_R \tau) [H^0 - iA^0]] , \tag{6}
\end{aligned}$$

where in the second line we have explicitly taken the large  $m_A$  ( $\alpha \rightarrow \beta - \pi/2$ ) and large  $\tan\beta$  limits. The flavour-diagonal muon coupling to MSSM Higgs bosons [22] in these limits is given by

$$\mathcal{L}_{\mu\text{-Higgs}} = \frac{e}{\sin\theta_W} \frac{m_\mu}{2m_W} \bar{\mu} [h^0 + \tan\beta H^0 - i \tan\beta \gamma^5 A^0] \mu , \tag{7}$$

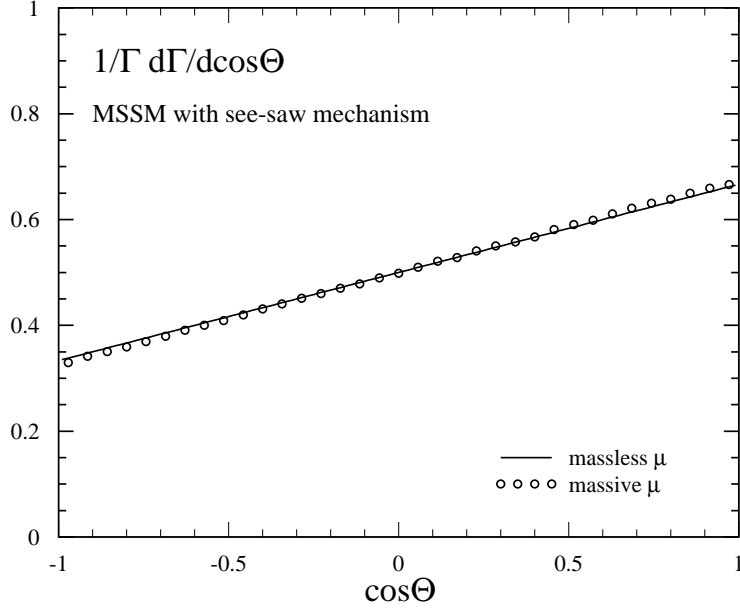


Figure 2:  $1/\Gamma \, d\Gamma/d\cos\Theta$  for the supersymmetric see–saw model with large  $\tan\beta$  defined in Ref. [11]. We display the analytic result obtained for massless muons together with the numerical calculation including all mass effects.

so integrating out the  $H^0$  and  $A^0$  fields leads to the relevant part of the effective Lagrangian given by

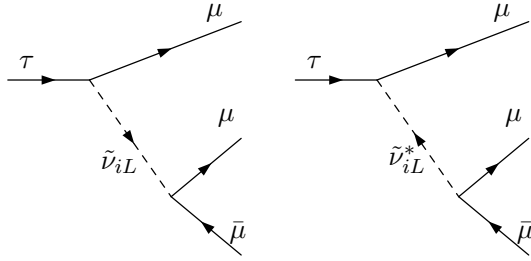
$$\begin{aligned}
\mathcal{L}_{\text{eff}} &= -(2G_F^2)^{1/4} m_\tau \kappa_{32}^* (\tan\beta)^2 \frac{e}{\sin\theta_W} \frac{m_\mu}{2m_W} (\bar{\mu} P_R \tau) \bar{\mu} \left[ \frac{1}{m_{H^0}^2} \tan\beta - \tan\beta \gamma^5 \frac{1}{m_A^2} \right] \mu \\
&= -(2G_F^2)^{1/4} m_\tau \kappa_{32}^* (\tan\beta)^3 \frac{e}{\sin\theta_W} \frac{m_\mu}{2m_W} \frac{2}{m_A^2} (\bar{\mu} P_L \mu) (\bar{\mu} P_R \tau). \tag{8}
\end{aligned}$$

In the second line of (8) we have used the fact that in the large  $m_A$  limit, the mass of the heavier  $CP$ –even Higgs boson,  $H^0$ , is approximately equal to  $m_A$ . We can easily see that the only non–zero effective coupling  $g_{ab}^c$  in the Lagrangian (1) is  $g_{RR}^S$ , which we set to 1.

Performing the phase–space integrations analytically with massless muons gives the result

$$\frac{1}{\Gamma} \frac{d\Gamma}{d\cos\Theta} = \frac{3 + \cos\Theta}{6}, \tag{9}$$

which can be derived from Eq. (4) and (5). In order to quantify the effect of muon masses, we display Eq.(9) in Fig. 2, along with the result of a numerical calculation incorporating massive muons. As expected, the muon mass effects are very small. A Monte–Carlo simulation of the decay  $\tau \rightarrow \mu\mu\bar{\mu}$  within the MSSM see–saw model for a typical LHC general purpose detector (with cuts as described in Section 1) shows an acceptance of 30%.



(plus diagrams with the muons crossed.)

Figure 3: Feynman diagrams leading to  $\tau \rightarrow \mu\mu\bar{\mu}$  in the MSSM without  $R$ -parity.

### 3.2 Supersymmetric model with $R$ -parity violation

The MSSM without  $R$ -parity (see *e.g.* Refs. [23] for reviews) includes an additional set of Yukawa interactions, between the charged leptons and sneutrinos, which are not necessarily diagonalized when the Higgs-lepton Yukawa interactions are diagonalized, allowing for the possibility of charged-lepton-flavour-violation by a scalar particle at tree-level. The  $R$ -parity-violating part of the superpotential is given by

$$W_{\mathcal{R}_p} = \epsilon_{ab} \left( \frac{1}{2} \lambda_{ijk} L_i^a L_j^b \bar{E}_k + \lambda'_{ijk} L_i^a Q_j^b \bar{D}_k + \kappa_i L_i^a H_u^b \right) + \frac{1}{2} \epsilon_{rst} \lambda''_{ijk} \bar{U}_i^r \bar{D}_j^s \bar{D}_k^t. \quad (10)$$

Here,  $i, j, k = 1, 2, 3$  are generation indices,  $a, b = 1, 2$  are  $SU(2)$  and  $r, s, t = 1, 2, 3$  are  $SU(3)$  indices.  $L, \bar{E}$  denote the lepton doublet and singlet left-chiral superfields;  $Q, \bar{U}, \bar{D}$  denote the quark doublet and singlet superfields, respectively.  $\lambda, \lambda', \lambda''$  are dimensionless coupling constants and  $\kappa$  is a mass mixing parameter.

The terms relevant to the decay  $\tau \rightarrow \mu\mu\bar{\mu}$  are  $\epsilon_{ab} \frac{1}{2} \lambda_{ijk} L_i^a L_j^b \bar{E}_k$  plus its Hermitian conjugate, which give interaction terms  $\lambda_{i23} \tilde{\nu}_{iL} \bar{\mu} P_R \tau$ ,  $\lambda_{i32}^* \tilde{\nu}_{iL}^* \bar{\mu} P_L \tau$ ,  $\lambda_{i22} \tilde{\nu}_{iL} \bar{\mu} P_R \mu$  and  $\lambda_{i22}^* \tilde{\nu}_{iL}^* \bar{\mu} P_L \mu$ . These lead to the  $\tau \rightarrow \mu\mu\bar{\mu}$  diagrams shown in Fig. 3. Integrating out the sneutrinos, which are constrained to be heavy ( $m_{\tilde{\nu}} \gg m_\tau$ ), gives the following terms in the effective Lagrangian:

$$\mathcal{L}_{\text{eff}} = \sum_i \left( \frac{1}{m_{\tilde{\nu}_{iL}}^2} \lambda_{i32} \lambda_{i22}^* (\bar{\mu} P_R \mu) (\bar{\mu} P_L \tau) + \frac{1}{m_{\tilde{\nu}_{iL}}^2} \lambda_{i22} \lambda_{i23}^* (\bar{\mu} P_L \mu) (\bar{\mu} P_R \tau) \right), \quad (11)$$

from which we can read off that  $g_{LL}^S$  is proportional to  $\lambda_{i32} \lambda_{i22}^*$  and  $g_{RR}^S$  is proportional to  $\lambda_{i22} \lambda_{i23}^*$ ,  $g_{LR}^S = g_{RL}^S = 0$ , and all the vector and tensor couplings are also zero.

Bottom-up approaches to constraining the MSSM without  $R$ -parity generally consider the minimal number of couplings to be non-zero for any individual constraining process [24], *e.g.* constraints from the current upper bound on  $\tau \rightarrow \mu\mu\bar{\mu}$  assume either  $\lambda_{i32} \lambda_{i22}^* \neq 0$  and  $\lambda_{i22} \lambda_{i23}^* = 0$  or the other way around, to obtain a conservative upper bound in the absence of destructive interference [25]. Here we take two benchmark scenarios: one where  $g_{LL}^S = 1$  and  $g_{RR}^S = 0$ , designated “L”, and the other where



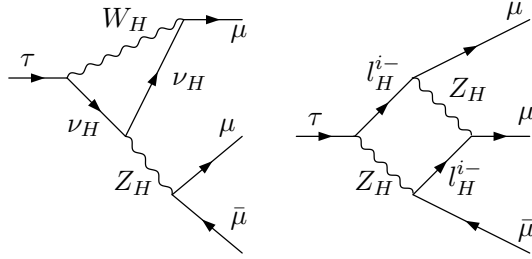


Figure 4: Example Feynman diagrams leading to  $\tau \rightarrow \mu\mu\bar{\mu}$  in the Littlest Higgs model with  $T$ -parity. For the full set, see Ref. [27].

$g_{LL}^S = 0$  and  $g_{RR}^S = 1$ , designated “R”. If the decay  $\tau \rightarrow \mu\mu\bar{\mu}$  is measurable at the LHC because this model is correct, then it is almost certain that it will have been established from other signals, and the measurement distinguishing between the two benchmarks would be most useful for measuring the  $R$ -parity-violating couplings.

Performing the phase-space integrations analytically with massless muons gives the result

$$\frac{1}{\Gamma} \frac{d\Gamma}{d\cos\Theta} = \begin{cases} \frac{3 - \cos\Theta}{6} & \text{for L: } g_{LL}^S = 1, g_{RR}^S = 0, \\ \frac{3 + \cos\Theta}{6} & \text{for R: } g_{LL}^S = 0, g_{RR}^S = 1. \end{cases} \quad (12)$$

Simulation of these decays for a typical LHC general purpose detector shows an acceptance of 25% and 30% for “L” and “R”, respectively.

### 3.3 Littlest Higgs model with $T$ -parity

The additional gauge group(s) and fermion multiplets in the Littlest Higgs model with  $T$ -parity (LHT model) (see *e.g.* Refs. [26]) allow for flavour-changing interactions through loops of  $T$ -odd particles with potentially very different PMNS- or CKM-like matrices. We focus on the way this allows for  $\tau \rightarrow \mu\mu\bar{\mu}$  decays as discussed in Ref. [27].

We start directly from equations (5.2), (5.3) and (5.4) in Ref. [27], which give four-point amplitudes for  $\tau \rightarrow \mu\mu\bar{\mu}$  in the LHT. We reproduce them here for ease of reference:

$$\mathcal{A}_{\gamma'} = \frac{G_F}{\sqrt{2}} \frac{e^2}{8\pi^2} \frac{1}{q^2} \bar{D}'_{\text{odd}}{}^{\tau\mu} [\bar{\mu}(p_1) (m_\tau i\sigma_{\alpha\beta} q^\beta (1 + \gamma_5)) \tau(p)] [\bar{\mu}(p_2) \gamma^\alpha \mu(p_3)] - (p_1 \leftrightarrow p_2), \quad (13)$$

$$\mathcal{A}_\gamma = - \left[ 4 \frac{G_F}{\sqrt{2}} \frac{e^2}{8\pi^2} \bar{Z}'_{\text{odd}}{}^{\tau\mu} [\bar{\mu}(p_1) \gamma_\alpha (1 - \gamma_5) \tau(p)] [\bar{\mu}(p_2) \gamma^\alpha \mu(p_3)] - (p_1 \leftrightarrow p_2) \right], \quad (14)$$

$$\mathcal{A}_{\text{box}} = 2 \frac{G_F}{\sqrt{2}} \frac{\alpha}{2\pi \sin^2 \theta_W} \bar{Y}'_{\mu, \text{odd}}{}^{\tau\mu} [\bar{\mu}(p_1) \gamma_\alpha (1 - \gamma_5) \tau(p)] [\bar{\mu}(p_2) \gamma^\alpha (1 - \gamma_5) \mu(p_3)]. \quad (15)$$

The structure of the amplitude  $\mathcal{A}_\gamma$  corresponds to setting the couplings  $g_{LL}^V = g_{RL}^V = 1$  (and all others to zero) in the general effective Lagrangian (1), while the structure of the amplitude  $\mathcal{A}_{\text{box}}$  corresponds

to setting  $g_{RL}^V = 1$  and all other couplings to zero. The amplitude  $\mathcal{A}_{\gamma'}$  is already tightly constrained by  $\tau \rightarrow \mu\gamma$ , so we ignore it in the following. [We also found for input mirror-lepton to mirror- $W$  boson mass ratios in the range from 0.1 to 10 that  $\mathcal{A}_{\gamma'}$  is much smaller than the other amplitudes.] The functions  $\bar{Z}'_{\text{odd}}{}^{\tau\mu}$  and  $\bar{Y}'_{\mu,\text{odd}}{}^{\tau\mu}$ , defined in Ref. [27], encode all the information from the  $T$ -odd particles in the decay, and can vary strongly in their relative magnitude. However, we found that for mirror-lepton to mirror- $W$  mass ratios below 2,  $\bar{Z}'_{\text{odd}}{}^{\tau\mu} \ll \bar{Y}'_{\mu,\text{odd}}{}^{\tau\mu}$  while for ratios above about 4  $\bar{Z}'_{\text{odd}}{}^{\tau\mu}$  becomes dominant. As a pair of benchmarks, we thus take  $\bar{Z}'_{\text{odd}}{}^{\tau\mu} \gg \bar{Y}'_{\mu,\text{odd}}{}^{\tau\mu}$ , so  $g_{LL}^V = g_{RL}^V = 1$  (and all other couplings set to zero), designated “Z”, and  $\bar{Z}'_{\text{odd}}{}^{\tau\mu} \ll \bar{Y}'_{\mu,\text{odd}}{}^{\tau\mu}$ , so  $g_{RL}^V = 1$  and all others zero, designated “Y”.

Performing the phase-space integrations analytically with massless muons gives the result

$$\frac{1}{\Gamma} \frac{d\Gamma}{d\cos\Theta} = \begin{cases} \frac{9 + 5\cos\Theta}{18} & \text{for Z: } g_{LL}^V = 1, g_{RL}^V = 1, \\ \frac{1 + \cos\Theta}{2} & \text{for Y: } g_{LL}^V = 0, g_{RL}^V = 1. \end{cases} \quad (16)$$

Simulation of these decays in the LHC environment show an acceptance of 27% for both the scenarios “Z” and “Y”.

### 3.4 Topcolour-assisted technicolour model

Topcolour-assisted technicolour models [14], are based on the product of gauge groups  $SU(3)_1 \times SU(3)_2 \times U(1)_{Y1} \times U(1)_{Y2} \times SU(2)_L$  which is broken to  $SU(3)_{\text{QCD}} \times U(1)_{\text{EM}}$ . The group  $SU(3)_2 \times U(1)_{Y2}$  couples preferentially to the lighter two generations, while  $SU(3)_1 \times U(1)_{Y1}$  couples preferentially to the heaviest generation. The generation-dependence of the couplings lead in general to flavour-non-diagonal couplings of the heavy  $Z'$  vector gauge boson associated with the broken  $U(1)$  gauge group once the fermions have been diagonalized to the mass-eigenstate basis.

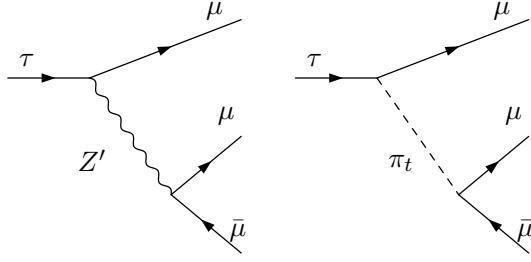
The top-pion,  $\pi_t$ , a condensate which breaks the  $SU(2)_L$  vacuum, can also mediate flavour-changing interactions. Since both the  $Z'$  and the top-pion masses and couplings are unknowns, we consider the two extreme cases where either of the two particles dominates the decay: we designate the  $Z'$  case by “Z” and the top-pion case by “P”, which occur for example when  $m_{\pi_t} \gg m_{Z'}$  or  $m_{\pi_t} \ll m_{Z'}$ , respectively.

We consider  $\tau \rightarrow \mu\mu\bar{\mu}$  through the heavy  $Z'$ , using couplings as given in Ref. [28]. The flavour-diagonal couplings read

$$\begin{aligned} \mathcal{L}_{Z'}^{\text{FD}} &= -\frac{1}{2}g_1 \cot\theta' Z'_\mu (\bar{\tau}_L \gamma^\mu \tau_L + 2\bar{\tau}_R \gamma^\mu \tau_R) \\ &\quad -\frac{1}{2}g_1 \tan\theta' Z'_\mu (\bar{\mu}_L \gamma^\mu \mu_L + 2\bar{\mu}_R \gamma^\mu \mu_R + \bar{e}_L \gamma^\mu e_L + 2\bar{e}_R \gamma^\mu e_R), \end{aligned} \quad (17)$$

while the flavour-changing couplings are given by

$$\begin{aligned} \mathcal{L}_{Z'}^{\text{FC}} &= -\frac{1}{2}g_1 Z'_\mu [k_{\tau\mu} (\bar{\tau}_L \gamma^\mu \mu_L + 2\bar{\tau}_R \gamma^\mu \mu_R) + k_{\tau e} (\bar{\tau}_L \gamma^\mu e_L + 2\bar{\tau}_R \gamma^\mu e_R) \\ &\quad + k_{\mu e} \tan^2\theta' Z'_\mu (\bar{\mu}_L \gamma^\mu \mu_L + 2\bar{\mu}_R \gamma^\mu \mu_R + \bar{e}_L \gamma^\mu e_L + 2\bar{e}_R \gamma^\mu e_R)] + \text{h.c.}, \end{aligned} \quad (18)$$



(plus diagrams with the muons crossed.)

Figure 5: Feynman diagrams leading to  $\tau \rightarrow \mu\mu\bar{\mu}$  in the topcolour–assisted technicolour model.

where  $g_1 = \sqrt{4\pi\alpha}/\cos\theta_W$  and  $\theta'$  is the mixing angle<sup>2</sup> for the heavy  $Z'$ . The  $k_{lij}$  are flavour mixing factors.

Integrating out the  $Z'$  gives the following relevant terms in the effective Lagrangian:

$$\begin{aligned} \mathcal{L}_{\text{eff}} = & \frac{1}{m_{Z'}^2} \frac{\pi\alpha}{(\cos\theta_W)^2} \tan\theta' k_{\tau\mu} (\bar{\mu}\gamma^\mu P_L \mu \bar{\mu}\gamma^\mu P_L \tau + 2\bar{\mu}\gamma^\mu P_R \mu \bar{\mu}\gamma^\mu P_L \tau \\ & + 2\bar{\mu}\gamma^\mu P_L \mu \bar{\mu}\gamma^\mu P_R \tau + 4\bar{\mu}\gamma^\mu P_R \mu \bar{\mu}\gamma^\mu P_R \tau) , \end{aligned} \quad (19)$$

from which we can read off that  $g_{RL}^V = 1$ ,  $g_{LL}^V = g_{RR}^V = 2$ ,  $g_{LR}^V = 4$  and all other couplings are zero.

Now we consider  $\tau \rightarrow \mu\mu\bar{\mu}$  through the  $\pi_t$ , using couplings as given in Ref. [29]. The couplings to the top–pion are given by the following terms in the Lagrangian:

$$\begin{aligned} \mathcal{L}_{\pi_t}^{\text{FD}} = & \left[ \frac{m_t}{\sqrt{2}F_t} \frac{\sqrt{\nu_\omega^2 - F_t^2}}{\nu_\omega} [K_{UR}^{tt} K_{UL}^{tt*} \bar{t}\gamma^5 t \pi_t^0 + \frac{m_b - m'_b}{m_t} \bar{b}\gamma^5 b \pi_t^0 + K_{UR}^{tc} K_{UL}^{tt*} \bar{t}L\gamma^5 c_R \pi_t^0] \right. \\ & \left. + \frac{m_l}{\sqrt{2}\nu_\omega} \bar{l}\gamma^5 l \pi_t^0 + \frac{m_l}{\sqrt{2}\nu_\omega} K_{\tau i} \bar{\tau}\gamma^5 l_i \pi_t^0 \right] + \text{h.c.} , \end{aligned} \quad (20)$$

where  $m'_b \sim 0.1\epsilon m_t$  is the part of the bottom quark mass generated by extended technicolour ( $\epsilon \ll 1$  is a small parameter). The symbol  $K$  denotes flavour mixing factors,  $\nu_\omega = v/\sqrt{2}$  where  $v \simeq 246$  GeV is the scale of electroweak symmetry breaking and  $F_t$  is the top–pion decay constant.

Integrating out the  $\pi_t$  gives the following relevant terms in the effective Lagrangian:

$$\begin{aligned} \mathcal{L}_{\text{eff}} = & -\frac{m_l m_l}{2\nu_\omega^2} K_{\tau i}^* \bar{l}_j \gamma^5 l_j \bar{l}_i \gamma^5 \tau \\ = & -\frac{m_l m_l}{2\nu_\omega^2} K_{\tau i}^* \bar{l}_j (P_R - P_L) l_j \bar{l}_i (P_R - P_L) \tau , \end{aligned} \quad (21)$$

from which we can read off that  $g_{LL}^S = g_{RR}^S = 1$ ,  $g_{RL}^S = g_{LR}^S = -1$ , and all others are zero.

<sup>2</sup>We note that, in Ref. [28], the formula for the flavour–changing terms actually has  $\tan^2\theta$  rather than  $\tan^2\theta'$ , but we assume that this was a typographical error. We also assume that the Hermitian conjugate was also meant to be present in the equation. However, we disagree with equation (4) in Ref. [28], where we believe that the numerical factor should be 7/4096 rather than 25/384 for the case of identical particles in the final state ( $\tau \rightarrow \mu\mu\bar{\mu}, \mu\mu\bar{e}, e\mu\bar{e}, ee\bar{e}$ ) and 25/1536 for the case of no identical particles in the final state ( $\tau \rightarrow \mu e \bar{\mu}, \mu e \bar{e}$ ).

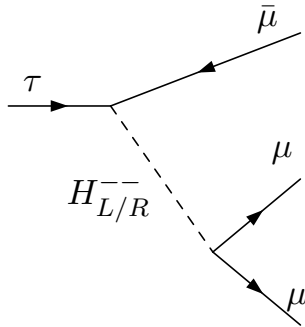


Figure 6: Feynman diagram leading to  $\tau \rightarrow \mu\mu\bar{\mu}$  in models with doubly-charged Higgs bosons.

Performing the phase-space integrations analytically with massless muons gives the result

$$\frac{1}{\Gamma} \frac{d\Gamma}{d\cos\Theta} = \begin{cases} \frac{7 - 5\cos\Theta}{14} & \text{for Z: } g_{RL}^V = 1, g_{LL}^V = g_{RR}^V = 2, g_{LR}^V = 4, \\ \frac{1}{2} & \text{for P: } g_{LL}^S = g_{RR}^S = 1, g_{RL}^S = g_{LR}^S = -1. \end{cases} \quad (22)$$

Simulation of  $\tau \rightarrow \mu\mu\bar{\mu}$  decays within the topcolour-assisted technicolour model show an acceptance of 29% and 28% for the “Z” and “P” scenarios, respectively.

### 3.5 Models with doubly-charged Higgs bosons

Models with doubly-charged Higgs bosons can mediate LFV  $\tau$  decays through Feynman diagrams like that depicted in Fig. 6. To be specific, we discuss two concrete models, the Higgs Triplet model [15], and the Zee-Babu model [16], both of which have been discussed in the context of LFV  $\tau$  decays previously in Ref. [17].

In the Higgs-triplet model neutrinos are given Majorana masses through the addition of a triplet of  $SU(2)$  with hypercharge 2 (no right-handed neutrinos are introduced) which obtains a vacuum expectation value. The doubly-charged components of this triplet can also mediate the decay  $\tau \rightarrow \mu\mu\bar{\mu}$ .

The Zee-Babu model [16] is another model in which neutrinos are given Majorana masses without the introduction of right-handed neutrinos, through the introduction of additional singly- and doubly-charged scalars which are singlets of  $SU(2)$ . The neutrino masses are generated radiatively at the two-loop level.

We start our discussion from equation (61) in Ref. [17] combined with Table 2 therein. We reproduce the (Hermitian conjugate of the) equation and the relevant information from the table here for ease of reference:

$$\mathcal{L}_{\text{eff}} = \left\{ \frac{-4G_F}{\sqrt{2}} g_3^* (\bar{\mu}\gamma^\nu P_R \mu) (\bar{\mu}\gamma_\nu P_R \tau) + g_4^* (\bar{\mu}\gamma^\nu P_L \mu) (\bar{\mu}\gamma_\nu P_L \tau) \right\}, \quad (23)$$

where

$$\frac{-4G_F}{\sqrt{2}}g_3 = 0 \quad \text{and} \quad \frac{-4G_F}{\sqrt{2}}g_4 = \frac{h_{\mu\mu}h_{\tau\mu}^*}{M_{H_L^{\pm\pm}}^2} \quad (24)$$

for the Higgs triplet model, and

$$\frac{-4G_F}{\sqrt{2}}g_3 = \frac{h_{\mu\mu}h_{\tau\mu}^*}{M_{H_R^{\pm\pm}}^2} \quad \text{and} \quad \frac{-4G_F}{\sqrt{2}}g_4 = 0 \quad (25)$$

for the Zee–Babu model. The constants  $h$  are mixing factors and  $M_{H_{L/R}^{\pm\pm}}$  is the mass of the doubly-charged scalar boson mediating the decay.

The structure of Eq. (23) to (25) corresponds to setting  $g_{RL}^V = 1$  and all other couplings to zero for the Higgs triplet model, while the  $g_{LR}^V = 1$  is the only non-zero coupling in the Zee–Babu model. We note that LFV  $\tau$  decays with a chirality structure analogous to that of the Higgs triplet model are predicted in seesaw models with scalar triplets, see *e.g.* Ref. [30].

Performing the phase-space integrations analytically with massless muons gives the result

$$\frac{1}{\Gamma} \frac{d\Gamma}{d\cos\Theta} = \begin{cases} \frac{1 + \cos\Theta}{2} & \text{for the Higgs triplet model: } g_{RL}^V = 1, \\ \frac{1 - \cos\Theta}{2} & \text{for the Zee–Babu model: } g_{LR}^V = 1. \end{cases} \quad (26)$$

Simulation of this decay for a typical LHC general purpose detector shows an acceptance of 25% and 30% for the Higgs triplet and Zee–Babu models, respectively.

## 3.6 Other Models

Finally, let us very briefly discuss some other new physics models, namely those that fit the criterion of heavy mediating particles, but have no concrete predictions for the dependence on  $\cos\Theta$ , those which are very constrained by the  $\tau \rightarrow \mu\gamma$  data, and unparticle models.

### 3.6.1 Heavy-particle-mediated

Left–Right Symmetric models [31] introduce a second  $SU(2)$  gauge group for the right-handed fermions, arranging them in appropriate doublets. The scalar sector is more complex than that of the SM, consisting of a Higgs bi-doublet and a Higgs triplet for each gauge group. The doubly-charged components of the triplets can mediate lepton flavour violation [17], but we find that the model is not predictive enough to meaningfully differentiate it through  $\Theta$ : the slope of  $1/\Gamma \, d\Gamma/d\cos\Theta$  depends on which  $H^{\pm\pm}$  dominates the decay and on the mixing matrices, which are entirely unknown in the right-handed sector.

### 3.6.2 Photon-mediated

Any model that predicts lepton flavour violation through loops will predict  $\tau \rightarrow \mu\mu\bar{\mu}$  through a virtual photon. However, unless the model predicts other processes that can facilitate  $\tau \rightarrow \mu\mu\bar{\mu}$  (such as the

see-saw MSSM), the bounds from  $\tau \rightarrow \mu\gamma$  mean that  $\tau \rightarrow \mu\mu\bar{\mu}$  from such models can barely be observed at LHC, let alone with sufficient statistics to discriminate models through angular distributions.

### 3.6.3 Unparticle-mediated

The phenomenology of “unparticles” [32] has recently attracted a considerable amount of attention. In particular, Refs. [33] and [34] consider the effects of unparticles mediating lepton flavour violation. However, the hypothesized unparticle sector has no predicted form for the couplings to the SM particles, and so has no unique effect on  $d\Gamma/d\cos\Theta$ . The unparticle nature of  $\tau \rightarrow \mu\mu\bar{\mu}$  would instead show up in the differential cross-section with respect to the energies of the muons, analogously to the analysis of the electron energies in Ref. [34].

## 3.7 Discrimination potential at the LHC

We summarize our results for the differential decay distributions  $1/\Gamma d\Gamma/d\cos\Theta$  within the various new physics models of Section 3 in Fig. 7, 8 and 9 and Tab. 1. [While Fig. 7, 8 and 9 display the numerical results including all mass effects, Tab. 1 quotes the analytic results for massless muons, which are an excellent approximation to the numerical calculation with full mass dependence.] We can see that determining the slope to within 10% should be sufficient to distinguish between the see-saw MSSM, the Littlest Higgs model with  $T$ -parity and the topcolour-assisted technicolour model. The  $R$ -parity-violating MSSM is not distinguishable from the see-saw MSSM for  $\lambda_{i22}\lambda_{i23}^*$  much larger than  $\lambda_{i32}\lambda_{i22}^*$ , but is easily discriminated from the Littlest Higgs model with  $T$ -parity and the topcolour-assisted technicolour model, since the magnitude of the slope is bounded by 1/6, which is less than the slopes of the other models.

With an estimated  $2 \times 10^8$   $\tau$  leptons produced from  $W$  bosons in the first year of low-luminosity operation of the LHC, the current upper bound on  $\tau \rightarrow \mu\mu\bar{\mu}$  means that even if the branching ratio is just below the bound and the full detector efficiency is not much lower than the simulated acceptance, we only expect about ten events in the first twelve months. However, after a year of high-luminosity operation, we expect as much as a hundred events, which should be sufficient to measure the  $\cos\Theta$  dependence of the decay width to within the desired 10%.

## 4 Conclusion

We have analyzed the lepton-flavour violating decay  $\tau \rightarrow \mu\mu\bar{\mu}$  and presented analytic expressions for the differential decay width derived from an effective Lagrangian with general four-fermion interactions. The results have been used in a Monte Carlo study to estimate the experimental acceptance of  $\tau \rightarrow \mu\mu\bar{\mu}$  decays at the LHC for generic sets of models. We have derived specific predictions for five classes of

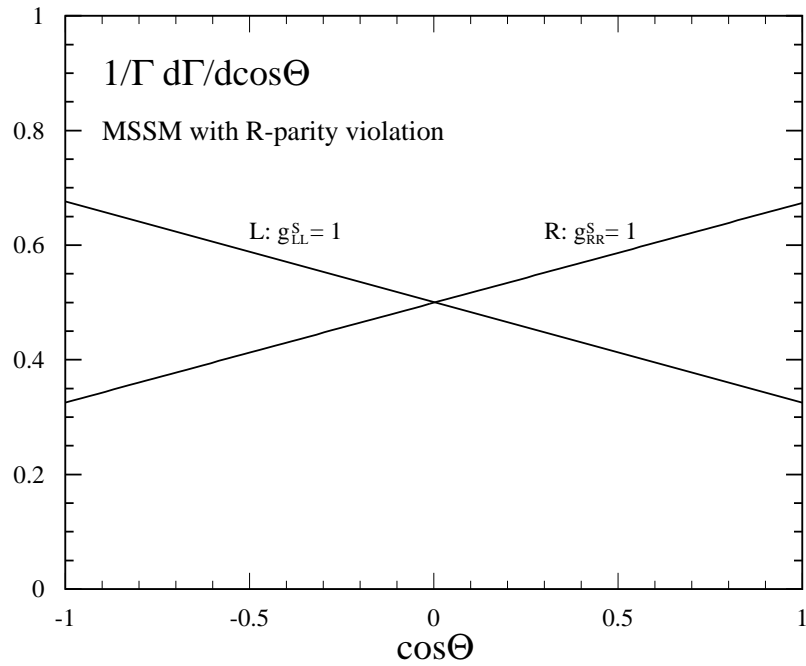
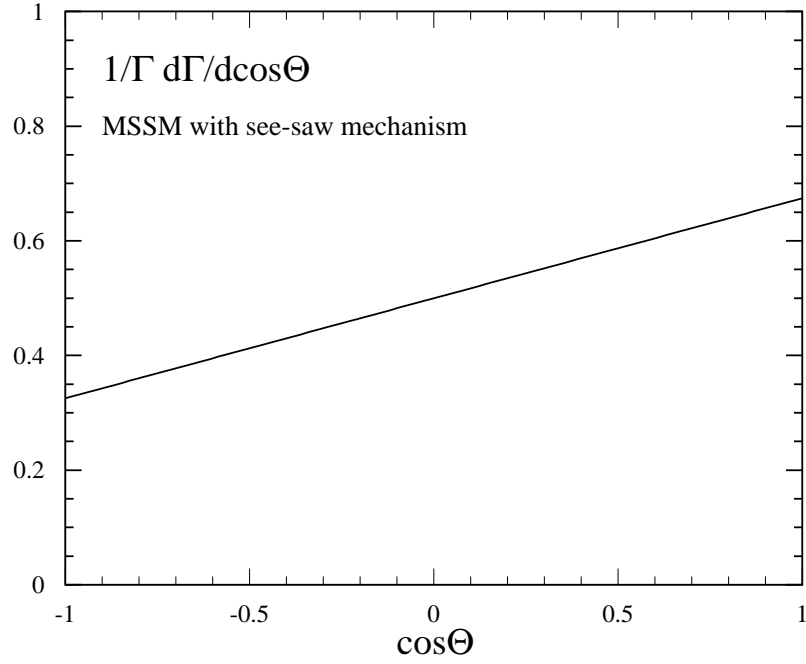


Figure 7:  $1/\Gamma \, d\Gamma/d\cos\Theta$  for the supersymmetric models with see-saw mechanism (upper figure) and  $R$ -parity violation (lower figure) discussed in Section 3. The results are obtained from a numerical calculation including all mass effects.

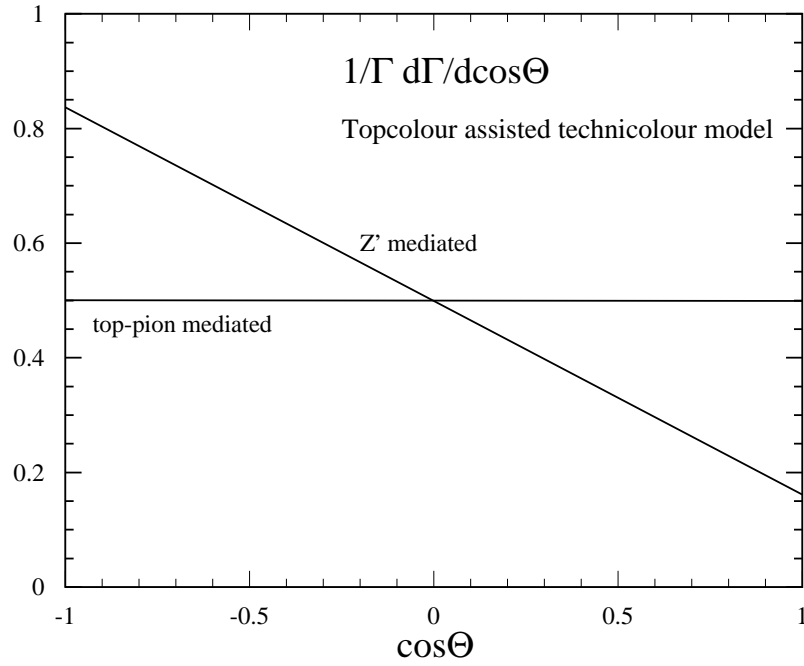
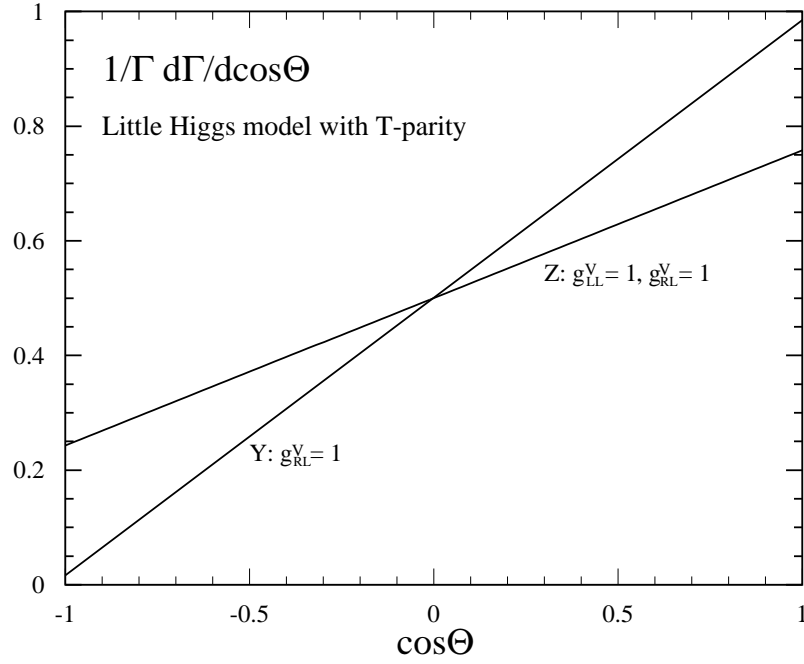


Figure 8:  $1/\Gamma d\Gamma/d\cos\Theta$  for the Littlest Higgs model (upper figure) and the topcolour–assisted technicolour model (lower figure) discussed in Section 3. The results are obtained from a numerical calculation including all mass effects.



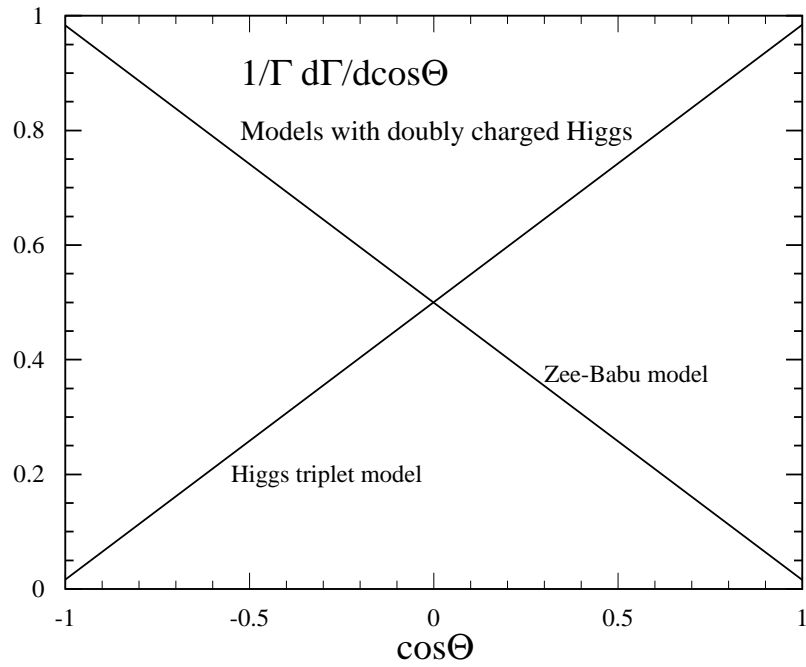


Figure 9:  $1/\Gamma \frac{d\Gamma}{d\cos\Theta}$  for the models with doubly-charged Higgs bosons discussed in Section 3. The results are obtained from a numerical calculation including all mass effects.

Model	$\frac{1}{\Gamma} \frac{d\Gamma}{d \cos \Theta} \propto 1 + A \cos \Theta$
MSSM with see-saw mechanism	$A = 1/6$
MSSM with $R$ -parity violation: “R” ( $\lambda_{i22}\lambda_{i23}^* \gg \lambda_{i32}\lambda_{i22}^*$ ) “L” ( $\lambda_{i22}\lambda_{i23}^* \ll \lambda_{i32}\lambda_{i22}^*$ )	$A = 1/6$ $A = -1/6$
Littlest Higgs model with $T$ -parity: “Z” ( $\bar{Z}'_{\text{odd}}{}^{\tau\mu} \gg \bar{Y}'_{\mu,\text{odd}}{}^{\tau\mu}$ ) “Y” ( $\bar{Z}'_{\text{odd}}{}^{\tau\mu} \ll \bar{Y}'_{\mu,\text{odd}}{}^{\tau\mu}$ )	$A = 5/18$ $A = 1/2$
Topcolour-assisted technicolour: “Z” ( $m_{\pi_t} \gg m_{Z'}$ ) “P” ( $m_{\pi_t} \ll m_{Z'}$ )	$A = -5/14$ $A = 0$
Models with doubly-charged Higgs bosons: Higgs triplet model Zee-Babu model	$A = 1/2$ $A = -1/2$

Table 1: The slope of  $1/\Gamma \, d\Gamma/d \cos \Theta$  for the various new physics models discussed in Section 3. The numbers are obtained from the analytic results for massless muons.

new physics models which predict the decay  $\tau \rightarrow \mu\mu\bar{\mu}$  at rates that may be observable at the LHC: the  $R$ -parity-conserving MSSM including see-saw neutrino masses at large  $\tan \beta$ , the  $R$ -parity-violating MSSM, the Littlest Higgs model with  $T$ -parity, the topcolour-assisted technicolour model, and models with doubly-charged Higgs bosons. For these models, our Monte Carlo studies of the decay  $\tau \rightarrow \mu\mu\bar{\mu}$  at the LHC predict experimental acceptances of approximately 25–30%. We have emphasized that the models can be distinguished from each other by measuring the angle between the  $\tau$  polarization vector and the momentum of the anti-muon. This can be achieved within a year of full luminosity at the LHC, if the branching ratio for the decay  $\tau \rightarrow \mu\mu\bar{\mu}$  is close to its current upper bound.

## Acknowledgments

We would like to thank Tord Riemann for discussions on LFV violating decays in the SM. The work of M.K. and B.O’L. was supported in part by the DFG grant KR 3345/1-1 and by the DFG SFB/TR9 “Computational Particle Physics”. The work of M.G. was supported in part by the BMBF grant FSP2-CMS.

## References

- [1] W. M. Yao *et al.* [Particle Data Group], J. Phys. G **33** (2006) 1 and 2007 partial update for the 2008 edition.
- [2] B. W. Lee and R. E. Shrock, Phys. Rev. D **16** (1977) 1444; T. P. Cheng and L. F. Li, Phys. Rev. Lett. **45** (1980) 1908; G. Mann and T. Riemann, Annalen Phys. **40** (1984) 334; J. I. Illana and T. Riemann, Phys. Rev. D **63** (2001) 053004 [arXiv:hep-ph/0010193].
- [3] N. G. Unel, arXiv:hep-ex/0505030.
- [4] F. Deppisch, H. Pas, A. Redelbach, R. Rückl and Y. Shimizu, Phys. Rev. D **69** (2004) 054014 [arXiv:hep-ph/0310053]; W. Porod and W. Majerotto, Phys. Rev. D **66** (2002) 015003 [arXiv:hep-ph/0201284].
- [5] M. Sher and I. Turan, Phys. Rev. D **69** (2004) 017302 [arXiv:hep-ph/0309183].
- [6] R. Santinelli and M. Biasini, CMS Note 2002/037.
- [7] K. Abe *et al.* [Belle Collaboration], arXiv:0708.3272 [hep-ex]; B. Aubert *et al.* [BABAR Collaboration], arXiv:0708.3650 [hep-ex].
- [8] see *e.g.* “SuperB: A high-luminosity heavy flavour factory. Conceptual design report,”, arXiv:0709.0451 [hep-ex].
- [9] R. Kitano and Y. Okada, Phys. Rev. D **63** (2001) 113003 [arXiv:hep-ph/0012040]; A. Matsuzaki and A. I. Sanda, arXiv:0711.0792 [hep-ph]; D. Black, T. Han, H. J. He and M. Sher, Phys. Rev. D **66** (2002) 053002 [arXiv:hep-ph/0206056]; B. M. Dassinger, T. Feldmann, T. Mannel and S. Turczyk, JHEP **0710** (2007) 039 [arXiv:0707.0988 [hep-ph]].
- [10] For example: J. A. Casas and A. Ibarra, Nucl. Phys. B **618** (2001) 171 [arXiv:hep-ph/0103065]; A. Dedes, J. R. Ellis and M. Raidal, Phys. Lett. B **549** (2002) 159 [arXiv:hep-ph/0209207]; A. Brignole and A. Rossi, Nucl. Phys. B **701** (2004) 3 [arXiv:hep-ph/0404211]; E. Arganda and M. J. Herrero, Phys. Rev. D **73** (2006) 055003 [arXiv:hep-ph/0510405].
- [11] K. S. Babu and C. Kolda, Phys. Rev. Lett. **89** (2002) 241802 [arXiv:hep-ph/0206310].
- [12] I. Hinchliffe and T. Kaeding, Phys. Rev. D **47** (1993) 279; B. de Carlos and P. L. White, Phys. Rev. D **54** (1996) 3427 [arXiv:hep-ph/9602381].
- [13] H. C. Cheng and I. Low, JHEP **0309** (2003) 051 [arXiv:hep-ph/0308199]; H. C. Cheng and I. Low, JHEP **0408** (2004) 061 [arXiv:hep-ph/0405243].

- [14] C. T. Hill, Phys. Lett. B **345** (1995) 483 [arXiv:hep-ph/9411426]; K. D. Lane and E. Eichten, Phys. Lett. B **352** (1995) 382 [arXiv:hep-ph/9503433]; K. D. Lane, Phys. Lett. B **433** (1998) 96 [arXiv:hep-ph/9805254].
- [15] J. Schechter and J. W. F. Valle, Phys. Rev. D **22** (1980) 2227; G. B. Gelmini and M. Roncadelli, Phys. Lett. B **99** (1981) 411; doubly charged
- [16] A. Zee, Nucl. Phys. B **264** (1986) 99; K. S. Babu, Phys. Lett. B **203** (1988) 132.
- [17] A. G. Akeroyd, M. Aoki and Y. Okada, Phys. Rev. D **76** (2007) 013004 [arXiv:hep-ph/0610344].
- [18] M. Gell-Mann, P. Ramond and R. Slansky, Print-80-0576 (CERN)
- [19] S. F. King, Rept. Prog. Phys. **67** (2004) 107 [arXiv:hep-ph/0310204].
- [20] F. Borzumati and A. Masiero, Phys. Rev. Lett. **57** (1986) 961.
- [21] L. J. Hall, V. A. Kostelecky and S. Raby, Nucl. Phys. B **267** (1986) 415.
- [22] J. Rosiek, arXiv:hep-ph/9511250, erratum for: J. Rosiek, Phys. Rev. D **41** (1990) 3464.
- [23] H. K. Dreiner, arXiv:hep-ph/9707435; R. Barbier *et al.*, Phys. Rept. **420** (2005) 1 [arXiv:hep-ph/0406039].
- [24] For example: V. D. Barger, G. F. Giudice and T. Han, Phys. Rev. D **40** (1989) 2987; D. Choudhury and P. Roy, Phys. Lett. B **378** (1996) 153 [arXiv:hep-ph/9603363]; J. P. Saha and A. Kundu, Phys. Rev. D **66** (2002) 054021 [arXiv:hep-ph/0205046]; J. E. Kim, P. Ko and D. G. Lee, Phys. Rev. D **56** (1997) 100 [arXiv:hep-ph/9701381]; J. H. Jang, J. K. Kim and J. S. Lee, Phys. Rev. D **55** (1997) 7296 [arXiv:hep-ph/9701283]; H. K. Dreiner, G. Polesello and M. Thormeier, Phys. Rev. D **65** (2002) 115006 [arXiv:hep-ph/0112228].
- [25] H. K. Dreiner, M. Krämer and B. O’Leary, Phys. Rev. D **75** (2007) 114016 [arXiv:hep-ph/0612278].
- [26] J. Hubisz and P. Meade, Phys. Rev. D **71** (2005) 035016 [arXiv:hep-ph/0411264]; N. Arkani-Hamed, A. G. Cohen, E. Katz, A. E. Nelson, T. Gregoire and J. G. Wacker, JHEP **0208** (2002) 021 [arXiv:hep-ph/0206020]; H. C. Cheng and I. Low, JHEP **0309** (2003) 051 [arXiv:hep-ph/0308199].
- [27] M. Blanke, A. J. Buras, B. Duling, A. Poschenrieder and C. Tarantino, JHEP **0705** (2007) 013 [arXiv:hep-ph/0702136].
- [28] C. x. Yue, Y. m. Zhang and L. j. Liu, Phys. Lett. B **547** (2002) 252 [arXiv:hep-ph/0209291].
- [29] C. X. Yue, Z. J. Zong, L. Zhou and S. Yang, Phys. Rev. D **71** (2005) 115011 [arXiv:hep-ph/0506070].

- [30] A. Abada, C. Biggio, F. Bonnet, M. B. Gavela and T. Hambye, *JHEP* **0712** (2007) 061 [arXiv:0707.4058 [hep-ph]].
- [31] J. C. Pati and A. Salam, *Phys. Rev. D* **10** (1974) 275 [Erratum-ibid. *D* **11** (1975) 703]; R. N. Mohapatra and J. C. Pati, *Phys. Rev. D* **11** (1975) 2558; G. Senjanovic and R. N. Mohapatra, *Phys. Rev. D* **12** (1975) 1502.
- [32] H. Georgi, *Phys. Rev. Lett.* **98** (2007) 221601 [arXiv:hep-ph/0703260]; see also: J. J. van der Bij and S. Dilcher, *Phys. Lett. B* **655** (2007) 183 [arXiv:0707.1817 [hep-ph]]; M. Neubert, arXiv:0708.0036 [hep-ph].
- [33] T. M. Aliev, A. S. Cornell and N. Gaur, arXiv:0705.1326 [hep-ph].
- [34] D. Choudhury, D. K. Ghosh and Mamta, arXiv:0705.3637 [hep-ph].